

# Coordinated Multipoint Joint Transmission in Heterogeneous Networks

Gaurav Nigam, Paolo Minero, and Martin Haenggi

**Abstract**—Motivated by the ongoing discussion on coordinated multipoint in wireless cellular standard bodies, this paper considers the problem of base station cooperation in the downlink of heterogeneous cellular networks. The focus of the paper is the *joint transmission* scenario, where an ideal backhaul network allows a set of randomly located base stations, possibly belonging to different network tiers, to jointly transmit data, so as to mitigate intercell interference and hence improve coverage and spectral efficiency. Using tools from stochastic geometry, an integral expression for the network coverage probability is derived in the scenario where the typical user located at an arbitrary location, namely the general user, receives data from a pool of base stations that are selected based on their average received power levels. An expression for the coverage probability is also derived for the typical user located at the point equidistant from three base stations, which we refer to as the worst-case user. In the special case where cooperation is limited to two base stations, numerical evaluations illustrate absolute gains in coverage probability of up to about 17% for the general user and 24% for the worst-case user compared to the non-cooperative case. It is also shown that no diversity gain is achieved using non-coherent joint transmission while full diversity gain can be achieved at the receiver if the transmitting base stations have channel state information.

**Index Terms**—Base station cooperation, coverage probability, CoMP, diversity gain, heterogeneous networks, Poisson point process, stochastic geometry.

## I. INTRODUCTION

### A. Motivation

The wireless industry is currently facing an increasing demand for data traffic over cellular networks [1], just as the performance of modern point-to-point communication schemes are fast approaching the fundamental information-theoretic limits. Therefore, to address this increasing demand, one of the solutions for increasing network coverage and capacity is the deployment of heterogeneous networks—networks of small base stations (BSs) along with the existing macro ones. In order to address the additional intercell interference caused by such deployments, the most recent discussions in the LTE cellular standard bodies center around the proposals of coordinated multipoint (CoMP) techniques [2], where BSs communicate with each other over a backhaul link to limit the intercell interference and exploit the benefits of distributed

multiple antenna systems [3], hence increasing the network throughput. [4] and [5] support these claimed advantages of CoMP through simulations and field trials, respectively, whereas [2] and [6] evaluate different deployment scenarios and list the operational challenges in deploying CoMP. [7] provides a good survey of the literature related to cooperation in cellular networks.

### B. Related Work

The problem of base station cooperation in wireless networks has been extensively studied in the past few decades.

In the information-theoretic literature, several studies including [8]–[11] analyze the advantages of cooperation within the framework of the Wyner model [12] for downlink communication—a widely used model to analyze the capacity of cellular systems, which is also known to trade off simplicity and analytic tractability at the expense of accuracy [13]. We refer the reader to [14] for an overview on the information-theoretic techniques to study multi-cell MIMO cooperation in wireless networks. [15] provides a fundamental information-theoretic limit on the achievable spectral efficiency due to cooperation, which proves that we cannot achieve arbitrarily high rates using cooperation.

Another approach that has been recently followed by several authors is to assume that the BSs are *randomly* located, such that tools from stochastic geometry can be used to characterize the signal-to-interference-plus-noise-ratio (SINR) at the typical user and hence the outage/coverage probability, see, e.g., [16] and [17]. Following this approach, [18] models a heterogeneous network as the union of several tiers of BSs independently distributed in space according to a Poisson point processes (PPPs). [19] empirically validates this approach by comparing the coverage probability derived under this model and the one observed in a real network deployment. [20] analyzes the average rate in the downlink of a heterogeneous network and also lists out a number of references for existing studies under this model.

Several cooperation techniques have been studied in the literature. For example, [21] studies the impact of backhaul delays in wireless networks where CoMP takes the form of zero forcing beamforming at the cooperating BSs; [22] also investigates the effect of a non-ideal backhaul network and analyzes the performance of a specific two-base-station cooperative scheme based on rate-splitting, similar to the one proposed in [23] for the multiple access channel with conferencing encoders; [24] analyzes a scheme where random clusters of BSs cooperate by nulling the intercell interference. [25] also considers the problem of non-coherent joint

Manuscript date June 21, 2014.

Gaurav Nigam {gnigam@nd.edu}, Paolo Minero {pminero@nd.edu} and Martin Haenggi {mhaenggi@nd.edu} are with the Department of Electrical Engineering, University of Notre Dame, IN 46556, USA.

The paper was presented in part at the 2013 IEEE GLOBECOM Workshop on Emerging Technologies for LTE-Advanced and Beyond 4G.

This work was partially supported by the U.S. NSF grants CCF 1117728 and 1216407.

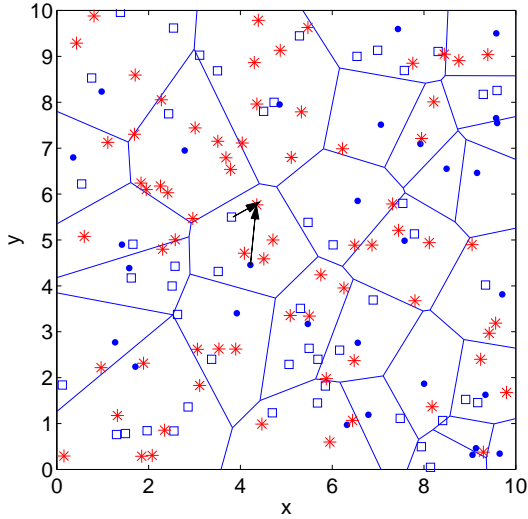


Fig. 1. Two-tier heterogeneous network with Voronoi cells of tier-1 where dots and squares denote the base stations from tier-1 and tier-2, respectively, and stars denote general users, which are uniformly distributed over the  $\mathbb{R}^2$  plane. In this case, the general user connects to  $n = 2$  base stations with strongest average received powers, denoted by arrows (Case 1).

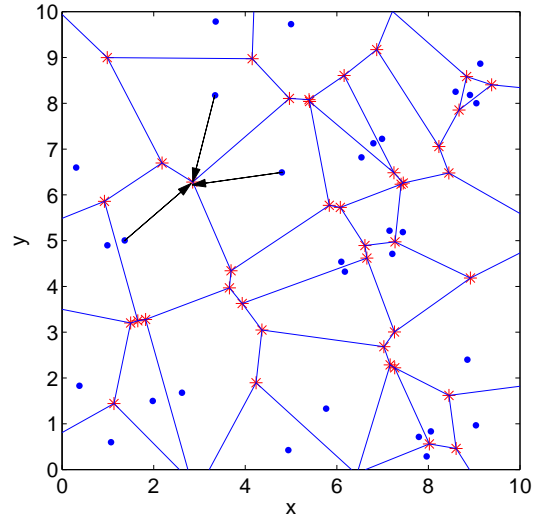


Fig. 2. Voronoi cells in a single-tier network where dots denote the base stations and stars denote worst-case users, which are located at Voronoi vertices. In this case, the worst-case user connects to (a subset of) the three equidistant BSs, denoted by arrows (Case 2).

transmission. However, the signal and interference powers are approximated to obtain a tractable problem, and the paper only focuses on general users. Unlike any of these existing works, this paper analyzes the benefits of joint transmission in heterogeneous networks for the general and worst-case users.

### C. Contributions

This paper presents a tractable stochastic geometry-based model for studying BS cooperation in the downlink of heterogeneous networks. The model consists of  $K$  independent tiers of randomly located BSs, where each tier is characterized by a different density of BSs and available power. Base stations within each tier are assumed to be spatially distributed according to a PPP. While this model can be used to analyze arbitrary cooperation schemes, the paper focuses on the *joint transmission* scenario, where BSs jointly transmit data to the same user in a synchronous manner, as if they were forming a single distributed antenna system. Assuming that cooperating BSs do not have channel state information<sup>1</sup> (CSI), and that a user connects to the set of BSs that results in the maximum average received power, we derive closed integral-form expressions for the coverage probability in two different cases:

- *Case 1:* The receiver is a *general user* in a heterogeneous network, i.e., it is located at an arbitrary location in the  $\mathbb{R}^2$  plane independent of the BS distribution process (see Fig. 1).
- *Case 2:* The receiver is a *worst-case user* in a single-tier network, i.e., it is located at a Voronoi vertex. A Voronoi vertex is a point that is equidistant from three BSs (see Fig. 2).

<sup>1</sup>Throughout the paper, we denote the phase shift due to fading as the channel state.

In both the cases described above, the expressions derived for the coverage probability illustrate the impact of the underlying network parameters, such as the density of BSs, the available transmit powers, and the fading coefficients, on the overall system performance. When specialized to the case of an interference-limited network, where the background noise is negligible compared to the interference power, in both cases the coverage probability becomes independent of the network tier density and available power, and in Case 1 it is also independent of number of network tiers.

We also study the diversity gain, defined as the rate of convergence to 1 of the coverage probability in the high coverage regime. We observe that in both cases, diversity gain is independent of the number of cooperating BSs because of the assumption that the transmitting BSs do not have CSI (see Theorem 3 and 4). In contrast, it is shown in Section IV-B that if the transmitting BSs have CSI, the diversity gain is equal to the number of cooperating BSs in both cases (see Theorem 5).

The results obtained are used to quantify the benefits of cooperation. A numerical evaluation of the case where cooperation is limited to two BSs illustrates absolute gains in coverage probability of up to about 17% for the general user and 24% for the worst-case user compared to the non-cooperative case (see Fig. 3 for  $\theta = 0$  dB).

### D. Paper Organization and Notations

This paper is organized as follows. Section II introduces the system model. Section III presents the main results, namely integral expressions for the coverage probabilities in the two cases described above. Section IV explores the diversity and power gains for coherent and non-coherent joint transmission. Section V discusses various assumptions made in the system model, extends some results derived in Section III, and includes numerical evaluations of the expressions derived to

illustrate the gains of cooperation over the non-cooperative case. Section VI concludes the paper.

Throughout we denote by  $\|\mathbf{u}\|_p$  the  $L^p$ -norm of a vector  $\mathbf{u} = (u_1, u_2, \dots, u_n) \in \mathbb{R}^n$ , i.e.,  $\|\mathbf{u}\|_p = (\sum_{i=1}^n |u_i|^p)^{1/p}$ , and we drop the subscript  $p$  in the special case  $p = 2$  of Euclidean distance. We denote the empty set by  $\emptyset$ . We use the tilde notation for asymptotic equivalence, i.e.,  $f(x) \sim g(x)$  as  $x \rightarrow a$  to mean  $\lim_{x \rightarrow a} f(x)/g(x) = 1$ .

## II. SYSTEM MODEL

### A. Heterogeneous Network Model

We consider a heterogeneous wireless network composed of  $K$  independent network tiers of BSs with different deployment densities and transmit powers. It is assumed that the BSs belonging to the  $i$ th tier have transmit power  $P_i$  and are spatially distributed according to a two-dimensional homogeneous PPP  $\Phi_i$  of density  $\lambda_i$ ,  $i = 1, \dots, K$ . We focus on the typical user. We assume without loss of generality that the typical user is located at the origin  $(0, 0) \in \mathbb{R}^2$  and a subset of the total ensemble of BSs cooperate by jointly transmitting a message to the typical user. We denote by  $\mathcal{C} \subset \bigcup_{i=1}^K \Phi_i$  the set of the cooperating BSs. In this setup, the received channel output at the typical user can be written as

$$\sum_{x \in \mathcal{C}} \frac{P_{\nu(x)}^{1/2}}{\|x\|^{\alpha/2}} h_x w_x X + \sum_{x \in \mathcal{C}^c} \frac{P_{\nu(x)}^{1/2}}{\|x\|^{\alpha/2}} h_x w_x X_x + Z, \quad (1)$$

where the first sum is the desired signal from the set of cooperating BSs, the second sum is the interference from the non-cooperating BSs, and  $Z$  is a standard additive circular symmetric complex white zero mean Gaussian random variable with variance  $\sigma^2$  modeling the background thermal noise;  $\nu(x)$  is the index of the network tier to which BS located at  $x \in \mathbb{R}^2$  belongs, i.e.,  $\nu(x) = i$  iff  $x \in \Phi_i$ ;  $h_x$  denotes the random fading coefficient between the BS located at  $x$  and the user located at the origin;  $w_x$  denotes the precoder used by BS located at  $x$ ;  $\alpha > 2$  denotes the path loss exponent;  $X$  denotes the channel input symbol that is sent by the cooperating BSs;  $\mathcal{C}^c := \bigcup_{i=1}^K \Phi_i \setminus \mathcal{C}$  denotes the BSs that are not in the set of cooperating BSs;  $X_x$  denotes the channel input symbol sent by the BS located at  $x \in \mathcal{C}^c$ . Throughout the paper it is assumed that the fading coefficients  $h_x$  are i.i.d. zero mean unit variance complex normal distributed random variables independent of everything else (Rayleigh fading), a legitimate assumption in a rich scattering environment. Depending on whether the BS located at  $x$  has CSI or not, the precoder  $w_x$  is set as:

$$w_x = \begin{cases} 1, & \text{no CSI;} \\ \frac{h_x^*}{|h_x|}, & \text{CSI,} \end{cases} \quad (2)$$

where  $h_x^*$  denotes the complex conjugate of  $h_x$ .

Assuming that the  $X_x$  and  $X$  in (1) are independent zero-mean random variables of unit variance, the SINR at the

typical user is given by

$$\begin{aligned} \text{SINR} &= \frac{\left| \sum_{x \in \mathcal{C}} P_{\nu(x)}^{1/2} \|x\|^{-\alpha/2} h_x w_x \right|^2}{\sum_{x \in \mathcal{C}^c} P_{\nu(x)} \|x\|^{-\alpha} |h_x w_x|^2 + \sigma^2} \\ &= \frac{\left| \sum_{x \in \mathcal{C}} P_{\nu(x)}^{1/2} \|x\|^{-\alpha/2} h_x w_x \right|^2}{\sum_{i=1}^K P_i I_i + \sigma^2} \end{aligned} \quad (3)$$

where we defined

$$I_i := \sum_{x \in \Phi_i \setminus \mathcal{C}} |h_x w_x|^2 \|x\|^{-\alpha}. \quad (4)$$

### B. General and Worst-case Users

We consider two types of users, based on their relative position with respect to the set of BSs:

- 1) *General user (Case 1)*: First, we consider the typical user in  $\mathbb{R}^2$  and assume that the set of cooperating BSs  $\mathcal{C}$  consists of the  $n$  BSs in  $\bigcup_{j=1}^K \Phi_j$  with the *strongest* average received power, where the average is taken with respect to the fading coefficient (see Fig. 1). More precisely,

$$\mathcal{C} = \arg \max_{\{x_1, \dots, x_n\} \subset \bigcup_{j=1}^K \Phi_j} \sum_{i=1}^n \frac{P_{\nu(x_i)}}{\|x_i\|^\alpha}. \quad (5)$$

Notice that the BSs in  $\mathcal{C}$  belong in general to different network tiers. This setup is applicable to heterogeneous wireless networks where users keep a list of the neighboring BSs with the strongest received power to initiate handoff requests.

- 2) *Worst-case user (Case 2)*: Second, we consider the typical cell-corner user. Specifically, we focus on the typical user located at a Voronoi vertex in a single-tier network  $\Phi$  distributed according to a homogeneous PPP with intensity  $\lambda$  and transmit power  $P$ . If  $\text{NP}_i(z)$  represents the distance between the location  $z$  and the  $i$ th nearest point in  $\Phi$ , then the set of Voronoi vertices for a given realization of  $\Phi$  is defined as

$$\mathcal{V} = \{z \in \mathbb{R}^2 : \text{NP}_1(z) = \text{NP}_2(z) = \text{NP}_3(z)\} \quad (6)$$

We select the worst-case user as the typical element of the set  $\mathcal{V}$  (averaged over  $\Phi$ ) and, without loss of generality, we assume the origin of the coordinate system to be at the location of the selected worst-case user. In this setup, we assume that the set of cooperating BSs  $\mathcal{C}$  is a subset of the 3 BSs in  $\Phi$  which are at equal distance from the origin. If we denote by  $x_i$  the location of the  $i$ -th closest BS to the origin, then

$$\mathcal{C} \subseteq \{x_1, x_2, x_3\}. \quad (7)$$

Notice that in both cases, given a number  $n$  of cooperating BSs, the set  $\mathcal{C}$  is uniquely determined almost surely.

### C. Performance Metrics

We restrict our attention on the following three performance metrics:

1) *Coverage probability*: Let  $|\mathcal{C}| = n$ . For a given threshold  $\theta$ , we define the coverage probability  $P_n$  at the typical user as

$$P_n = \mathbb{P}(\text{SINR} > \theta). \quad (8)$$

We refer to  $1 - P_n$  as outage probability and denote the coverage probability for the general user and the worst-case user as  $P_n^{\mathbb{R}^2}$  and  $P_n^{\mathcal{V}}$ , respectively, to emphasize the sets these two users belong to.

2) *Diversity gain*: As in [26, Definition 3], we define the diversity gain  $d_n$  as the rate of decay to zero of the outage probability  $1 - P_n$  in the high coverage regime, i.e.,

$$d_n = \lim_{\theta \rightarrow 0} \frac{\log(1 - P_n)}{\log \theta}. \quad (9)$$

We remark that our definition (9) is similar to the usual definition of diversity gain as the rate of decay to zero of the error probability in the high SNR regime [27, Equation 9.3].

3) *Power gain*: We define the power gain as the gain in SINR in the high coverage regime that can be achieved by  $n$  cooperating BSs relative to the no cooperation case, i.e.,

$$\frac{\left(\lim_{\theta \rightarrow 0} \frac{\theta^{d_n}}{1 - P_n}\right)^{1/d_n}}{\left(\lim_{\theta \rightarrow 0} \frac{\theta^{d_1}}{1 - P_1}\right)^{1/d_1}}. \quad (10)$$

The above definition implies that if, for instance,  $1 - P_n \sim (a_n \theta)^{d_n}$  as  $\theta \rightarrow 0$  for some  $a_n$  independent of  $\theta$ , then the power gain is  $a_1/a_n$ . The definition in (10) is similar to the usual definition of array gain in MIMO systems.

### III. COVERAGE PROBABILITIES

In this section, we assume that the BSs do not have CSI and thus  $w_x = 1$  for all  $x \in \bigcup_{i=1}^K \Phi_i$ . First, we derive an integral expression for the coverage probability (8) for the general user in Theorem 1. Second, we derive the coverage probability for the worst-case user in Theorem 2.

#### A. Case 1: General User

We prove the following result for the general user.

*Theorem 1*: For every  $n \geq 1$ ,

$$P_n^{\mathbb{R}^2} = \int_{\substack{0 < u_1 < \dots \\ \dots < u_n < \infty}} \exp\left(-u_n \left(1 + 2 \frac{F(\|\tilde{\mathbf{u}}\|_{\alpha/2}^{1/2} \theta^{-1/\alpha})}{\|\tilde{\mathbf{u}}\|_{\alpha/2} \theta^{-2/\alpha}}\right)\right) \times \exp\left(-\sigma^2 q^{-\alpha/2} \frac{\theta u_n^{\alpha/2}}{\|\tilde{\mathbf{u}}\|_{\alpha/2}^{\alpha/2}}\right) \mathbf{d}\mathbf{u}, \quad (11)$$

where  $\tilde{\mathbf{u}} = \left(\frac{u_n}{u_1}, \frac{u_n}{u_2}, \dots, \frac{u_n}{u_n}\right)$ ,

$$q = \pi \sum_{i=1}^K \lambda_i P_i^{2/\alpha}, \quad (12)$$

and

$$F(x) = \int_x^\infty \frac{r}{1+r^\alpha} dr. \quad (13)$$

*Proof*: See Appendix A. ■

*Remark 1*: Notice that the second exponential term in (11) approaches 1 as  $\sigma^2 \rightarrow 0$ . Using this fact, it can be shown that for small values of  $\sigma^2$  the coverage probability has asymptotic form

$$P_n^{\mathbb{R}^2} \sim \int_{\substack{0 < u_1 < \dots \\ \dots < u_n < \infty}} \exp\left(-u_n \left(1 + 2 \frac{F(\|\tilde{\mathbf{u}}\|_{\alpha/2}^{1/2} \theta^{-1/\alpha})}{\|\tilde{\mathbf{u}}\|_{\alpha/2} \theta^{-2/\alpha}}\right)\right) \mathbf{d}\mathbf{u}. \quad (14)$$

Quite remarkably, (14) shows that in the interference-limited regime where the background noise power is negligible compared to the interference power, the coverage probability at the general user becomes independent of the number of network tiers  $K$  and their respective power levels and deployment densities. A similar observation was made in [18, Eq. (3)] for non-cooperative interference-limited heterogeneous networks although in a slightly different setup. The intuition behind this result is that a variation in the number of network tiers or density of BSs leads to changes in the total received power as well as in the total aggregate interference power but in the absence of noise the scaling of these two quantities is such that their ratio remains constant.

*Remark 2*: Notice that  $P_n^{\mathbb{R}^2}$  depends on number of network tiers  $K$  and their respective transmit powers and deployment densities only through the variable  $q$  defined in (12).

*Remark 3*: The integral function  $F(x)$  defined in (13) cannot be solved explicitly in general, but closed-form expressions exist for specific values of  $\alpha > 2$ . In particular, it can be easily verified that if  $\alpha = 3$ , then

$$F(x) = \frac{1}{6} \log\left(1 + \frac{3x}{1-x+x^2}\right) + \frac{1}{\sqrt{3}} \tan^{-1}\left(\frac{\sqrt{3}}{2x-1}\right),$$

while

$$F(x) = \frac{1}{2} \tan^{-1}(x^{-2})$$

for  $\alpha = 4$ .  $F(x)$  can be expressed in terms of the hypergeometric function as [28]

$$F(x) = \frac{x^2}{(\alpha-2)(1+x^\alpha)} {}_2F_1(1, 1; 2-2/\alpha; 1/(1+x^\alpha)).$$

Using the above expression,

$$F(x) \sim \frac{x^{2-\alpha}}{\alpha-2}, \quad x \rightarrow \infty. \quad (15)$$

*Remark 4*: Theorem 1 generalizes several existing results in the literature. For instance, when specialized to the case  $\sigma^2 = 0$  and  $n = 1$ , (11) simplifies to

$$P_1^{\mathbb{R}^2} = \frac{1}{1 + 2\theta^{2/\alpha} F(\theta^{-1/\alpha})}, \quad (16)$$

thereby recovering the result in [29, Theorem 2] and [30, Corollary 2].

### B. Case 2: Worst-case User

We prove the following result for the worst-case user.

*Theorem 2:* For  $n = 1, 2, 3$ ,

$$P_n^{\mathcal{V}} = \int_0^\infty \frac{2d^3 \lambda^2 \pi^2 \left(1 + \frac{\theta}{n}\right)^{n-3} e^{-\sigma^2 \theta \frac{d^\alpha}{nP}}}{\exp\left(\lambda \pi d^2 \left(1 + 2 \frac{F((n/\theta)^{1/\alpha})}{(n/\theta)^{2/\alpha}}\right)\right)} dd. \quad (17)$$

*Proof:* See Appendix B. ■

*Remark 5:* In the interference-limited regime, the coverage probability for the worst-case user has asymptotic form

$$P_n^{\mathcal{V}} \sim \left(1 + \frac{\theta}{n}\right)^{n-3} \left(1 + 2 \left(\frac{\theta}{n}\right)^{2/\alpha} F\left(\left(\frac{\theta}{n}\right)^{-1/\alpha}\right)\right)^{-2}, \quad (18)$$

as  $\sigma^2 \rightarrow 0$ . As already remarked for the general user, (18) does not depend on the spatial density and available transmit power.

*Remark 6:* If  $n = 1$  and  $\sigma^2 = 0$ , (17) simplifies to

$$\begin{aligned} P_1^{\mathcal{V}} &= (1 + \theta)^{-2} \left(1 + 2\theta^{2/\alpha} F\left(\theta^{-1/\alpha}\right)\right)^{-2} \\ &= (1 + \theta)^{-2} \left(P_1^{\mathbb{R}^2}\right)^2, \end{aligned} \quad (19)$$

thereby recovering the result in [31, Proposition 1]. It follows from (19) that the coverage probability for the general user is higher than the one for the worst-case user. This is consistent with the fact that the general user is more likely to be in the coverage range of a BS than the cell-corner user. Equation (19) can be explained as follows: the factor  $(1 + \theta)^{-2}$  represents the loss in coverage probability due to the fact that the user is located at a point equidistant from three BSs, and that two of these BSs act as interferers; the second factor  $\left(P_1^{\mathbb{R}^2}\right)^2$  represents the loss due to the fact that the average distance between the typical Voronoi vertex and its nearest BS is  $3/2$  times the average distance between the typical location in the  $\mathbb{R}^2$  plane and its nearest BS.

## IV. DIVERSITY AND POWER GAIN

In this section we characterize the diversity gain and the power gain for general user and worst-case user under different CSI assumptions.

### A. Non-coherent Joint Transmission

If CSI is not available at the BSs, then the following result holds for the general user.

*Theorem 3:* For every  $n \geq 1$ , the diversity gain (9) for the general user is

$$d_n = 1, \quad (20)$$

and the power gain (10) is

$$\left(1 + \frac{\left(n! \frac{\Gamma(1+\frac{\alpha}{2})}{\Gamma(n+\frac{\alpha}{2})} - 1\right)}{1 + \sigma^2 q^{-\frac{\alpha}{2}} \left(\frac{\alpha}{2} - 1\right) \Gamma(1 + \frac{\alpha}{2})}\right)^{-1} \frac{\Gamma(1 + \frac{\alpha}{2})}{\phi_n(\alpha) \Gamma(n + \frac{\alpha}{2})}. \quad (21)$$

with

$$\phi_n(\alpha) = \int_{\substack{0 < t_1 < \dots \\ \dots < t_{n-1} < 1}} \frac{dt}{1 + \sum_{k=1}^{n-1} t_k^{-\alpha/2}}.$$

*Proof:* First, we derive an asymptotic form for the integrand in (11) in the high coverage regime. As  $\theta \rightarrow 0$

$$\begin{aligned} &\exp\left(-u_n \left(1 + 2 \frac{F\left(\|\tilde{\mathbf{u}}\|_{\alpha/2}^{1/2} \theta^{-1/\alpha}\right)}{\|\tilde{\mathbf{u}}\|_{\alpha/2} \theta^{-2/\alpha}}\right) - \frac{\sigma^2 \theta u_n^{\alpha/2}}{q^{\alpha/2} \|\tilde{\mathbf{u}}\|_{\alpha/2}^{\alpha/2}}\right) \\ &\stackrel{(a)}{\sim} \exp\left(-\frac{\frac{2u_n \theta}{\alpha-2} + \sigma^2 \theta u_n^{\alpha/2} q^{-\alpha/2}}{\|\tilde{\mathbf{u}}\|_{\alpha/2}^{\alpha/2}}\right) e^{-u_n} \\ &\stackrel{(b)}{\sim} \left(1 - \theta \frac{\frac{2u_n}{\alpha-2} + \sigma^2 u_n^{\alpha/2} q^{-\alpha/2}}{\|\tilde{\mathbf{u}}\|_{\alpha/2}^{\alpha/2}}\right) e^{-u_n} \end{aligned}$$

where (a) follows from (15) and the fact that  $\|\tilde{\mathbf{u}}\|_{\alpha/2}^{1/2} \theta^{-1/\alpha} \rightarrow \infty$  as  $\theta \rightarrow 0$ , while (b) uses the fact that  $e^{-x} \sim 1 - x$  as  $x \rightarrow 0$ . Next, notice that the integrand in (11) is bounded by the integrable function  $e^{-u_n}$ . Then, by the dominated convergence theorem (DCT)

$$\begin{aligned} P_n^{\mathbb{R}^2} &\sim \int_{\substack{0 < u_1 < \dots \\ \dots < u_n < \infty}} \left(1 - \theta \frac{\frac{2u_n}{\alpha-2} + \sigma^2 u_n^{\alpha/2} q^{-\alpha/2}}{\|\tilde{\mathbf{u}}\|_{\alpha/2}^{\alpha/2}}\right) e^{-u_n} d\mathbf{u} \\ &= 1 - \theta \int_{\substack{0 < u_1 < \dots \\ \dots < u_n < \infty}} \left(\frac{\frac{2u_n}{\alpha-2} + \sigma^2 u_n^{\alpha/2} q^{-\alpha/2}}{\|\tilde{\mathbf{u}}\|_{\alpha/2}^{\alpha/2}}\right) e^{-u_n} d\mathbf{u}. \end{aligned} \quad (22)$$

Notice that when  $n = 1$  (22) simplifies to

$$1 - P_1^{\mathbb{R}^2} \sim \theta \left(\frac{2}{\alpha-2} + \sigma^2 q^{-\alpha/2} \Gamma(1 + \alpha/2)\right). \quad (23)$$

since  $\|\tilde{\mathbf{u}}\|_{\alpha/2} = 1$ . If  $n > 1$ , instead, the change of variable  $t_i = u_i/u_n$  for  $1 \leq i \leq n-1$  yields

$$\begin{aligned} 1 - P_n^{\mathbb{R}^2} &\sim \theta \int_{\substack{0 < t_1 < \dots \\ \dots < t_{n-1} < 1}} \int_0^\infty \frac{\frac{2u_n}{\alpha-2} + \sigma^2 u_n^{\alpha/2} q^{-\alpha/2}}{1 + \sum_{k=1}^{n-1} t_k^{-\alpha/2}} \cdot \frac{u_n^{n-1}}{e^{u_n}} du_n dt \\ &= \theta \left(n! \frac{2}{\alpha-2} + \sigma^2 q^{-\alpha/2} \Gamma(n + \alpha/2)\right) \phi_n(\alpha). \end{aligned} \quad (24)$$

Finally, the claim follows by replacing the outage probabilities in (9) and (10) by the corresponding asymptotic forms (23) and (24). ■

Similarly, we prove the following result for the worst-case user.

*Theorem 4:* For  $n = 1, 2, 3$ , the diversity gain (9) for the worst-case user is

$$d_n = 1,$$

and the power gain (10) is

$$n \left(1 + (1-n) \left(\frac{2\alpha}{\alpha-2} + \sigma^2 \frac{\Gamma(\frac{\alpha}{2} + 2)}{P(\lambda\pi)^{\frac{\alpha}{2}}}\right)^{-1}\right)^{-1}. \quad (25)$$

*Proof:* Proceeding as in the proof of Theorem 3, we first derive an asymptotic form for the integrand in (17) in the high coverage regime and then apply the DCT to get an asymptotic form for the outage probability.

By the change of variable  $t = \lambda\pi d^2$ , (17) can be re-written as

$$\int_0^\infty \frac{\exp\left(-2t \frac{F((n/\theta)^{1/\alpha})}{(n/\theta)^{2/\alpha}} - \frac{\sigma^2 \theta (\lambda\pi)^{-\alpha/2} t^{\alpha/2}}{nP}\right)}{(1 + \theta/n)^{3-n}} te^{-t} dt. \quad (26)$$

As  $\theta \rightarrow 0$ ,

$$\begin{aligned} & \frac{\exp\left(-2t \frac{F((n/\theta)^{1/\alpha})}{(n/\theta)^{2/\alpha}} - \frac{\sigma^2 \theta (\lambda\pi)^{-\alpha/2} t^{\alpha/2}}{nP}\right)}{(1 + \theta/n)^{3-n}} te^{-t} \\ & \stackrel{(a)}{\sim} \frac{\exp\left(-\frac{2t\theta/n}{\alpha-2} - \frac{\sigma^2 \theta (\lambda\pi)^{-\alpha/2} t^{\alpha/2}}{nP}\right)}{(1 + \theta/n)^{3-n}} te^{-t} \\ & \stackrel{(b)}{\sim} \left(1 - \frac{\theta(3-n)}{n}\right) \left(1 - \frac{2t\theta/n}{\alpha-2} - \frac{\sigma^2 \theta t^{\alpha/2}}{nP(\lambda\pi)^{\alpha/2}}\right) te^{-t} \\ & \stackrel{(c)}{\sim} \left(1 - \frac{\theta}{n} \left(3-n + \frac{2t}{\alpha-2} + \frac{\sigma^2 t^{\alpha/2}}{P(\lambda\pi)^{\alpha/2}}\right)\right) te^{-t} \end{aligned}$$

where (a) follows from (15), (b) uses the asymptotic forms  $(1+x)^{-m} \sim 1 - mx$  and  $e^{-x} \sim 1 - x$  as  $x \rightarrow 0$ , while (c) is obtained by ignoring the terms with  $\theta^2$ . Notice that the integrand in (26) is bounded by the integrable function  $te^{-t}$ . Therefore, by the DCT

$$\begin{aligned} P_n^\nu & \sim \int_0^\infty \left(1 - \frac{\theta}{n} \left(3-n + \frac{2t}{\alpha-2} + \frac{\sigma^2 t^{\alpha/2}}{P(\lambda\pi)^{\alpha/2}}\right)\right) te^{-t} dt \\ & = 1 - \frac{\theta}{n} \int_0^\infty \left(3-n + \frac{2t}{\alpha-2} + \frac{\sigma^2 t^{\alpha/2}}{P(\lambda\pi)^{\alpha/2}}\right) te^{-t} dt, \end{aligned}$$

which implies that

$$1 - P_n^\nu \sim \frac{\theta}{n} \left(3-n + \frac{4}{\alpha-2} + \frac{\sigma^2 \Gamma(\alpha/2 + 2)}{P(\lambda\pi)^{\alpha/2}}\right). \quad (27)$$

Finally, the claim follows by replacing the outage probabilities in (9) and (10) by the asymptotic form (27). ■

*Remark 7:* It follows from Theorems 3 and 4 that the diversity gain is independent of the number of cooperating BSs when BSs do not have CSI. This result is a consequence of the fact that without CSI the signals of the cooperating BSs sum non-coherently at the typical user and therefore the combined signal is equivalent to a single fading coefficient with higher mean. Hence, we only get power gain due to the cooperation in this case.

Notice that while the power gain (21) at the general user can only be evaluated numerically, the power gain (25) at the worst-case user is in closed form. If  $\alpha = 4$  and  $\sigma^2 = 0$ , for instance, (21) evaluates to 1.00, 2.33 and 3.76 for  $n = 1, 2, 3$ , respectively, while (25) simplifies to 1, 8/3 and 6. This corresponds to a gain of 3.67 dB (4.26dB) for Case 1 (Case 2, respectively) when  $n$  increases from 1 to 2 and a gain of 2.08 dB (3.52 dB) when  $n$  increases from 2 to 3.

## B. Coherent Joint Transmission

If CSI is available at the transmitters, the following result holds.

*Theorem 5:* For every  $n \geq 1$ , the diversity gain (9) is equal to

$$d_n = n$$

at both the general user and the worst-case user.

*Proof:* We focus on Case 1; the result for Case 2 can be proved by following similar steps. If  $w_x = h_x^*/|h_x|$ , the numerator in (3) is the squared sum of independent Rayleigh distributed random variables with different parameters, and it can be written as:

$$\left| \sum_{x \in \mathcal{C}} P_{\nu(x)}^{1/2} \|x\|^{-\alpha/2} |h_x| \right|^2 = \left( \sum_{i=1}^n X_i \right)^2,$$

where  $X_i$  has pdf  $\frac{x}{M_i^2} e^{-x^2/2M_i^2}$ ,  $x \geq 0$  with  $M_i = P_{\nu(x_i)}^{1/2} \|x_i\|^{-\alpha/2}$ ,  $x_i \in \mathcal{C}$ . By defining  $J := \sum_{i=1}^n P_i I_i + \sigma^2$ , the outage probability can be written as

$$\begin{aligned} 1 - P_n & = \mathbb{P} \left( \left( \sum_{i=1}^n X_i \right)^2 < \theta J \right) \\ & = \mathbb{E}_{M_i, J} \left( \int_{\substack{x_1 \geq 0, \dots, x_n \geq 0 \\ \sum_{i=1}^n x_i < \sqrt{\theta J}}} \prod_{i=1}^n \frac{x_i}{M_i^2} e^{-x_i^2/2M_i^2} dx \right) \\ & \stackrel{(a)}{=} \theta^n \mathbb{E}_{M_i, J} \left( \int_{\substack{t_1 \geq 0, \dots, t_n \geq 0 \\ \sum_{i=1}^n t_i < 1}} J^n \prod_{i=1}^n \frac{t_i}{M_i^2} e^{-\theta J \frac{t_i^2}{2M_i^2}} dt \right). \end{aligned}$$

Here, (a) follows from the change of variable  $x_i = \sqrt{\theta J} t_i$ . Notice that as  $\theta \rightarrow 0$ ,

$$J^n \prod_{i=1}^n \frac{t_i}{M_i^2} e^{-\theta J \frac{t_i^2}{2M_i^2}} \sim J^n \prod_{i=1}^n \frac{t_i}{M_i^2}.$$

Then, by the DCT [32],

$$\begin{aligned} 1 - P_n & \sim \theta^n \mathbb{E}_{M_i, J} \left( J^n \prod_{i=1}^n M_i^{-2} \right) \int_{\substack{t_1 \geq 0, \dots, t_n \geq 0 \\ \sum_{i=1}^n t_i < 1}} \prod_{i=1}^n t_i dt \\ & \stackrel{(a)}{\sim} \frac{\theta^n \mathbb{E}_{M_i, J} \left( J^n \prod_{i=1}^n M_i^{-2} \right)}{(2n)!}, \end{aligned} \quad (28)$$

where (a) is due to [33, Equation 4.634] and the fact that  $\mathbb{E}_{M_i, J} \left( J^n \prod_{i=1}^n M_i^{-2} \right)$  is finite [32]. For Case 2, we can follow similar steps as above with equal  $M_i$ 's for  $i \leq 3$  since the cooperating BSs are at equal distances from the user and are transmitting with same power. Therefore, we get a diversity gain of  $n$  in both cases. ■

It follows from Theorem 5 that the diversity gain is equal to the number of cooperating BSs in case of coherent joint transmission— in contrast to the result for non-coherent joint transmission. For the worst-case user, the  $M_i$ 's are equal and therefore, the sum in the numerator of SINR behaves similar

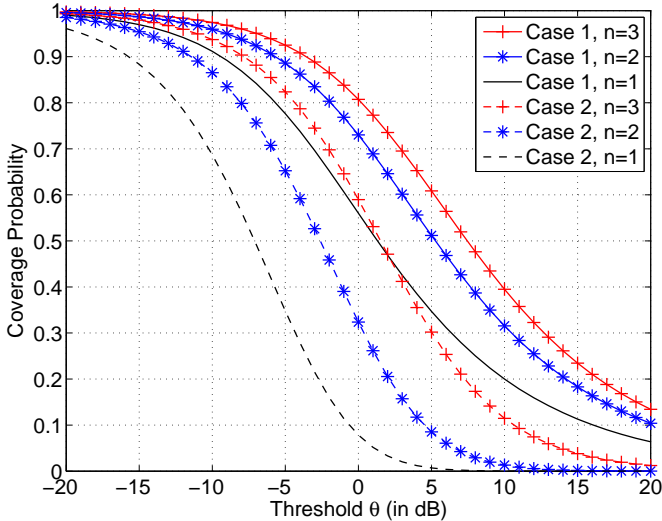


Fig. 3. Coverage probabilities evaluated using (11) and (17) for  $n = 1, 2, 3$  for the general user (Case 1) and the worst-case user (Case 2).

to a Nakagami- $n$  fading random variable. A similar result for the diversity gain has been derived in [34, Corollary 2] in the special case of Nakagami fading.

## V. DISCUSSION AND EXTENSIONS

In this section, we discuss the accuracy of some of the assumptions made in Section II, extend some of the results to more general scenarios, and present numerical evaluations of the integral expressions for the coverage probability derived in Section III. In all our numerical evaluations, we focus on the case of two network tiers consisting of a macro-tier overlaid with a pico-tier. Specifically, we assume that  $\alpha = 4$ ,  $\sigma^2 = 10^{-11}$ , and that the macro-tier has spatial intensity  $\lambda_1 = (500^2\pi)^{-1}$  and available power  $P_1 = 25$ , while the pico-tier has spatial intensity  $\lambda_2 = 5\lambda_1$  and available power  $P_2 = P_1/25 = 1$ .

### A. Coverage Probability and Effect of Thermal Noise

Fig. 3 plots the coverage probabilities (11) and (17) as a function of the threshold  $\theta$  for different values of  $n$ . We notice from this figure that at  $\theta = 0$  dB, the difference in the values of the coverage probability for  $n = 2$  and  $n = 1$  is 0.17 for the general user (Case 1) and 0.24 for the worst-case user (Case 2). These numbers demonstrate that the worst-case user benefits more from BS cooperation than the general user.

Fig. 4 compares the outage probabilities evaluated using (11) and (17) with the high-coverage-regime expressions given in (24) and (27), respectively. We observe that the asymptotic forms follow the outage probability curves very closely up to a threshold value of  $-15$  dB.

Fig. 5 illustrates the impact of the background thermal noise on the coverage probabilities (11) and (17), which are evaluated for  $\sigma^2 = 0$  and  $\sigma^2 = 10^{-11}$ . Notice that the curves with noise and without noise are close to each other, both for the general user (Case 1) and the worst-case user (Case 2), as predicted by (14) and (18).

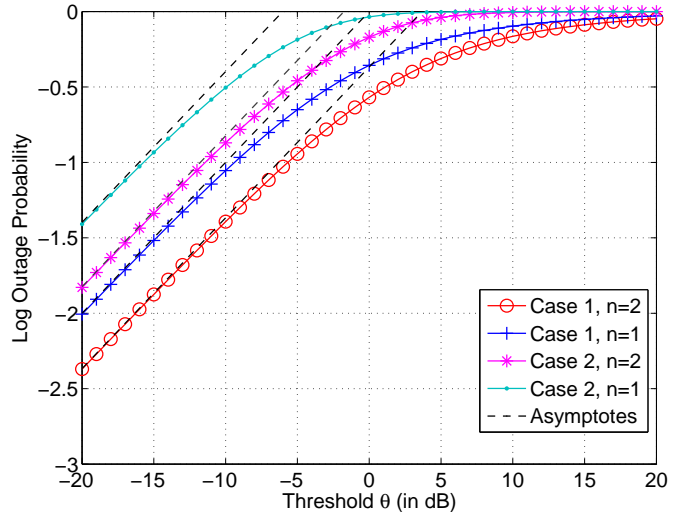


Fig. 4. Comparison between the outage probabilities evaluated using (11) and (17) and the asymptotic forms in (24) and (27) for  $n = 1, 2$ .

### B. Cooperation among Interferers

In (1) we assumed that the symbols transmitted by the interfering BSs in  $\mathcal{C}^c$  are mutually independent. In this subsection, we discuss the impact of this assumption on the derived coverage probability results. To do so, we consider a generalized model that accounts for cooperation among interferers. Specifically, we assume that symbol  $X_x$  is transmitted by a subset  $\mathcal{D} \subseteq \mathcal{C}^c$  of interfering BSs, such that the SINR at the typical user is given by

$$\text{SINR}_{\mathcal{D}} = \frac{\left| \sum_{x \in \mathcal{C}} P_{\nu(x)}^{1/2} \|x\|^{-\alpha/2} h_x w_x \right|^2}{I_{\mathcal{D}} + \sum_{x \in \mathcal{C}^c \setminus \mathcal{D}} P_{\nu(x)} \|x\|^{-\alpha} |h_x w_x|^2 + \sigma^2}, \quad (29)$$

where  $I_{\mathcal{D}} = \left| \sum_{x \in \mathcal{D}} P_{\nu(x)}^{1/2} \|x\|^{-\alpha/2} h_x w_x \right|^2$  denotes the interference power due to the cooperating interferers. Notice that (3) is recovered from (29) by setting  $\mathcal{D} = \emptyset$ . Assuming no CSI at the BSs, we prove the following result.

*Proposition 1:* Both in Case 1 and in Case 2, for every  $\mathcal{D} \subseteq \mathcal{C}^c$

$$\mathbb{P}(\text{SINR}_{\mathcal{D}} > \theta) \geq \mathbb{P}(\text{SINR}_{\emptyset} > \theta) = P_n, \quad (30)$$

with equality iff  $\mathcal{D} = \emptyset$ .

*Proof:* See Appendix C. ■

*Remark 8:* Proposition 1 proves that cooperation among interferers can only increase the coverage probability, hence the independence assumption made in (1) yields a lower bound on the coverage probability.

Loosely speaking, the result in Proposition 1 is a consequence of the fact that without CSI the signals of the cooperating interferers sum non-coherently at the typical user and therefore do not increase the mean interference power. The proof technique can be illustrated by focusing on a network realization with only two interferers. Without cooperation

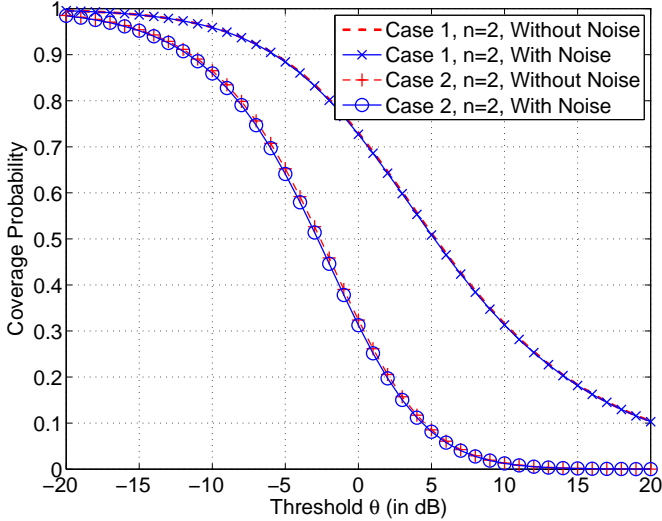


Fig. 5. Comparison between the coverage probabilities in (11) and (17) with  $\sigma^2 = 10^{-11}$  and the asymptotic forms in (14) and (18) for  $n = 2$ .

between them, the coverage probability at the typical user can be written as

$$\mathbb{P}\left(\frac{X_1}{X_2 + X_3 + \sigma^2} > \theta\right),$$

where  $X_1$ ,  $X_2$ , and  $X_3$  are independent exponential random variables because of the Rayleigh fading assumption. With cooperation between the interferers, instead, the coverage probability is given by

$$\mathbb{P}\left(\frac{X_1}{X_4 + \sigma^2} > \theta\right),$$

where  $X_4$  is independent of  $X_1$  and is exponentially distributed with mean  $\mathbb{E}(X_2) + \mathbb{E}(X_3)$ , because of the no CSI assumption. Notice that the mean interference power is the same in both cases. Moreover,

$$\begin{aligned} \mathbb{P}\left(\frac{X_1}{X_2 + X_3 + \sigma^2} > \theta\right) &= \mathbb{E}\left(e^{-\theta \frac{X_2 + X_3 + \sigma^2}{\mathbb{E}(X_1)}}\right) \\ &= \frac{e^{-\theta \frac{\sigma^2}{\mathbb{E}(X_1)}}}{\left(1 + \theta \frac{\mathbb{E}(X_2)}{\mathbb{E}(X_1)}\right)\left(1 + \theta \frac{\mathbb{E}(X_3)}{\mathbb{E}(X_1)}\right)} \\ &< \frac{e^{-\theta \frac{\sigma^2}{\mathbb{E}(X_1)}}}{1 + \theta \frac{\mathbb{E}(X_2) + \mathbb{E}(X_3)}{\mathbb{E}(X_1)}} \\ &= \mathbb{E}\left(e^{-\theta \frac{X_4 + \sigma^2}{\mathbb{E}(X_1)}}\right) \\ &= \mathbb{P}\left(\frac{X_1}{X_4 + \sigma^2} > \theta\right), \end{aligned}$$

which establishes the claimed result that cooperation between the interferers increases the coverage probability.

### C. Rate Gain

Now, we focus on the gain in the maximum achievable communication rate due to cooperation for a given coverage probability. For a fixed coverage probability  $p$ , substituting  $\theta$

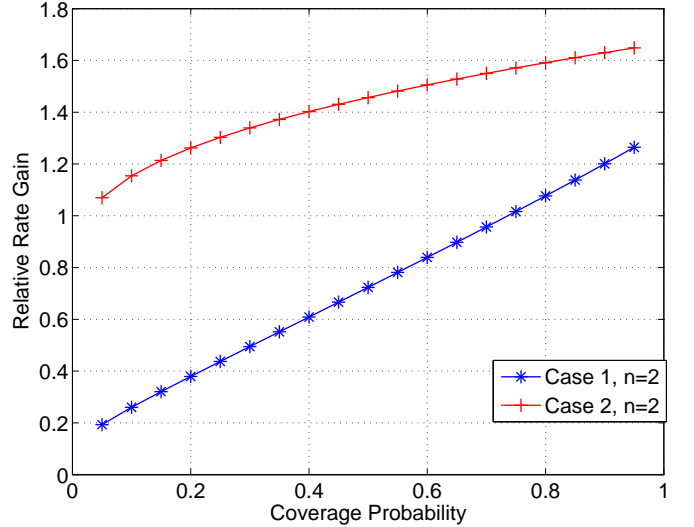


Fig. 6. Relative rate gain compared to no cooperation against fixed coverage probabilities for Case 1 and Case 2 with  $n = 2$  using (14), (16), (18), (19) and (31).

by  $2^R - 1$  in (14), (16), (18), and (19), setting the resulting expression equal to  $p$ , and solving for  $R$ , the expressions derived in Section III yield the maximum communication rates  $R^{(\text{wc},1)}(p)$ ,  $R^{(\text{nc},1)}(p)$ ,  $R^{(\text{wc},2)}(p)$ , and  $R^{(\text{nc},2)}(p)$  that can be achieved with probability  $p$  in Case 1 with and without cooperation and Case 2 with and without cooperation, respectively. Fig. 6 illustrates the relative rate *gain* for Case  $j$ ,  $j = 1, 2$ , over the no-cooperation case, which is computed as

$$\frac{R^{(\text{wc},j)}(p) - R^{(\text{nc},j)}(p)}{R^{(\text{nc},j)}(p)}, \quad j = 1, 2. \quad (31)$$

Notice that the rate gains provided by cooperation increase with  $p$  and when  $p \approx 1$  the relative gain is more than 110% in Case 1 and more than 160% in Case 2. If there was no cooperation, both the cooperating BSs would serve their own user and collectively they would achieve the rate  $2R^{(\text{nc},j)}(p)$ . Therefore, if they cooperate and serve one user together in one time-slot and other user in the next time-slot, they still achieve a higher rate than without cooperation, even for the general user.

### D. Heterogeneous Path Loss Exponents

Thus far, we have assumed a common path loss exponent  $\alpha$  across all network tiers. In practical developments, however, different networks operate in different propagation environments, e.g., macro BSs are typically located in an outdoor environment while femto BSs reside in an indoor setup. Therefore, it is realistic to assume that the path loss exponents are different across networks. In this subsection we consider this generalized setup, for which we prove the following result.

*Proposition 2:* If  $i$ th tier has a path loss exponent  $\alpha_i$ , the coverage probability  $P_n$  in (8) for the general user in an

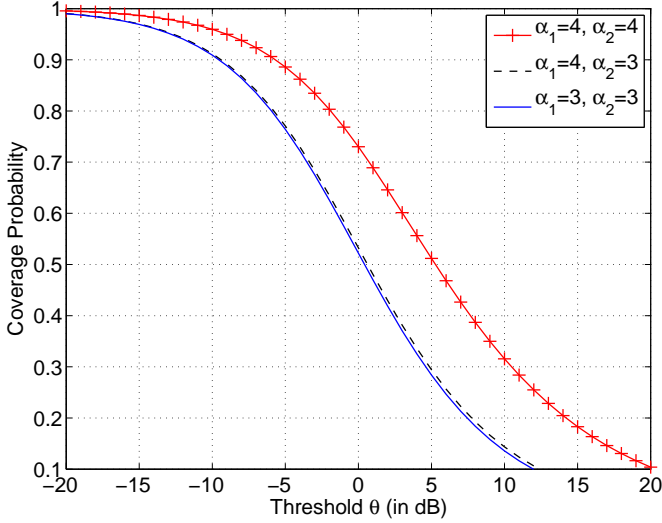


Fig. 7. Coverage probability in (32) for different path loss exponents  $\alpha_1, \alpha_2$  for each tier for  $n = 2$ .

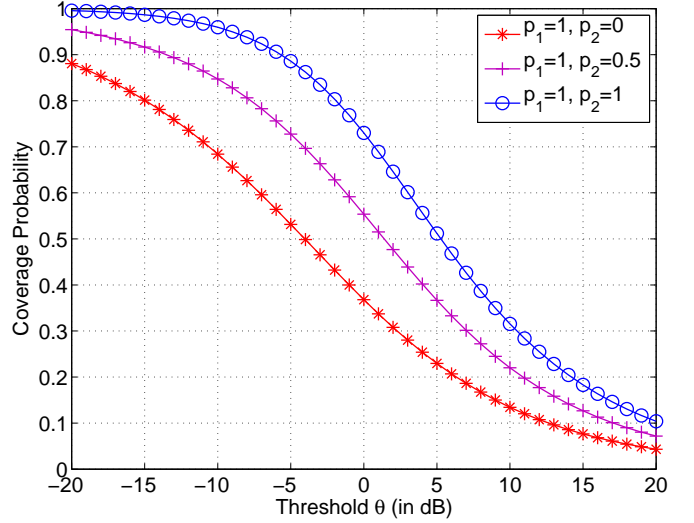


Fig. 8. Coverage probability in (34) for different tier-2 open-access probabilities  $p_2$  with  $p_1 = 1$  and  $n = 2$ .

interference-limited network is

$$\int_{0 < u_1 < \dots < u_n < \infty} \exp\left(-2\pi \sum_{i=1}^K \lambda_i (P_i u_n)^{\delta_i} \frac{F_i(\|\tilde{\mathbf{u}}\|_1^{\delta_i/2} \theta^{-\delta_i/2})}{\|\tilde{\mathbf{u}}\|_1^{\delta_i} \theta^{-\delta_i}}\right) \times f_{\mathbf{U}}(\mathbf{u}) d\mathbf{u} \quad (32)$$

where  $F_i(x) := \int_x^\infty \frac{r}{1+r^{\alpha_i}} dr$ ,  $\delta_i := 2/\alpha_i$  and

$$f_{\mathbf{U}}(\mathbf{u}) = e^{-\pi \sum_{i=1}^K \lambda_i P_i^{\delta_i} u_n^{\delta_i}} \prod_{i=1}^n \left( \sum_{j=1}^K \pi \lambda_j \delta_j P_j^{\delta_j} u_i^{\delta_j-1} \right) \quad (33)$$

*Remark 9:* Proposition 2 shows that the coverage probability depends on the tier intensities and powers even though  $\sigma^2 = 0$ , in contrast to the homogeneous path loss case (see Remark 1).

*Remark 10:* Notice that (14) is recovered from Proposition 2 by setting  $\alpha_i = \alpha$  for all  $i$ .

The proof of Proposition 2 follows closely the proof of Theorem 1 and therefore is omitted.

Notice that upper and lower bounds for (32) can be obtained by setting  $\alpha_i = \max_i \alpha_i$  for all  $i$  and  $\alpha_i = \min_i \alpha_i$  for all  $i$ , respectively. Fig. 7 shows the coverage probability assuming  $\alpha_1 = 4$  and  $\alpha_2 = 3$ , along with the corresponding upper bound ( $\alpha_1 = 4$  and  $\alpha_2 = 4$ ) and lower bound ( $\alpha_1 = 3$  and  $\alpha_2 = 3$ ). In this case the lower bound is tighter than the upper bound.

### E. Effect of Closed-Access BSs

So far we have assumed that all BSs in the network are available for cooperation. However, this assumption is not realistic in the presence of user-deployed femtocells that can be configured either in open-access mode, in which case they allow traffic from any nearby user, or in closed-access mode, in which case access is limited to a set of approved users.

The system model in Section II can be modified as proposed in [18] to allow for the presence of BSs operating in closed-access mode. Specifically, assume that each BS in  $i$ th tier is

in open-access mode with probability  $p_i$ , independently of all other BSs, and that cooperation can only take place among the BSs that are in open-access mode. Under these assumptions, the  $i$ th network tier can be partitioned as  $\Phi_i = \Phi_i^{(o)} + \Phi_i^{(c)}$ , where  $\Phi_i^{(o)}$  and  $\Phi_i^{(c)}$  denote the disjoint sets of open-access and closed-access BSs, respectively. By the thinning property of the PPP,  $\Phi_i^{(o)}$  and  $\Phi_i^{(c)}$  are distributed as independent homogeneous PPPs with intensities  $\lambda_i p_i$  and  $\lambda_i (1 - p_i)$ , respectively. Then, in Case 1 the set  $\mathcal{C}$  of cooperating BSs with closed-access BSs can be defined as in (5) with  $\Phi_i$  replaced by  $\Phi_i^{(o)}$ . In this setup, we prove the following result.

*Proposition 3:* If BSs in tier  $i$  are open-access with probability  $p_i$ , the coverage probability  $P_n$  in (8) for the general user in an interference-limited network is

$$\int_{0 < u_1 < \dots < u_n < \infty} \exp\left(-u_n \left(1 + G(\theta^{-1/\alpha} \|\tilde{\mathbf{u}}\|_{\alpha/2}^{1/2})\right)\right) d\mathbf{u}, \quad (34)$$

where

$$G(x) := \frac{2F(x)}{x^2} + \frac{1}{x^2 \text{sinc}(2/\alpha)} \frac{\sum_{i=1}^K \lambda_i (1 - p_i) P_i^{2/\alpha}}{\sum_{i=1}^K \lambda_i p_i P_i^{2/\alpha}}$$

*Proof:* See Appendix D. ■

*Remark 11:* Notice that (14) is recovered from Proposition 3 by setting  $p_i = 1$  for all  $i$ .

Fig. 8 shows the coverage probability at the general user assuming  $p_1 = 1$  at the macro-tier and different values of  $p_2$  at the pico-tier. The figure shows that at 0 dB decreasing  $p_2$  from 1 to 0 results in a loss of roughly 48% in coverage probability. This degradation is due to the additional interference caused by BSs that are in closed-access mode. The effect of nearby closed-access BSs can be mitigated using advanced-receiver techniques, such as successive interference cancellation [35], or network-assisted techniques, such as the use of almost blank subframes [36].

## VI. CONCLUSION

In this paper, we considered the problem of joint transmission in heterogeneous wireless networks. Using tools from stochastic geometry, we derived an integral expression for the coverage probability in two cases: 1) the general user in a heterogeneous network, located at the typical location in  $\mathbb{R}^2$  plane, and 2) the worst-case user in a single-tier network, located at the typical Voronoi vertex. The analysis for both the users is quite tractable and it shows that in the asymptotic regimes of low noise and high coverage, our derived integral expressions simplify and reveal that only a subset of network parameters are important in determining the coverage probability. Specifically, in case of interference-limited networks, the coverage probability becomes independent of the network tier densities and the available power for both the users. In the high coverage regime, the diversity gain for both the cases under non-coherent joint transmission is independent of the number of cooperating BSs, and full diversity gain is achieved with coherent joint transmission. Numerical results show that BS cooperation is more beneficial for the worst-case user compared to the general user. The analysis presented in this paper assumes that all BSs and the receiving user are equipped with a single antenna and symbols from all cooperating BSs are received synchronously at the receiver. Future work includes the generalization to the MIMO case as well as to the case where cooperating BSs have partial CSI.

### APPENDIX A PROOFS OF THEOREM 1

For every  $i = 1, \dots, K$ , let  $\Xi_i = \{\|x\|^\alpha/P_i, x \in \Phi_i\}$  denote the normalized path loss between each BS in  $\Phi_i$  and the typical user located at the origin. By the mapping theorem [37, Theorem 2.34],  $\Xi_i$  is a PPP with intensity  $\lambda_i(x) = \lambda_i \frac{2\pi}{\alpha} P_i^{2/\alpha} x^{2/\alpha-1}$ ,  $x \in \mathbb{R}^+$ . From the independence of the PPPs  $\Phi_1, \dots, \Phi_K$ , it follows that  $\Xi_1, \dots, \Xi_K$  are also independent and thus the process  $\Xi = \bigcup_{i=1}^K \Xi_i$  is a non-homogeneous PPP with density  $\lambda(x) = \sum_{i=1}^K \lambda_i(x)$ . Without loss of generality, suppose that the elements of  $\Xi$  are indexed in increasing order, such that  $\|x_1\|^\alpha/P_{\nu(x_1)} \leq \|x_2\|^\alpha/P_{\nu(x_2)} \leq \|x_3\|^\alpha/P_{\nu(x_3)} \leq \dots$ , and define

$$\gamma_k = \|x_k\|^\alpha/P_{\nu(x_k)} \quad (35)$$

as the normalized path loss between the typical user and the  $k$ -th BS in the ordered list. Since the typical user connects to the  $n$  BSs with the strongest average received power, it follows that  $\gamma = \{\gamma_1, \dots, \gamma_n\}$  denotes the normalized path loss of the cooperating BSs in  $\mathcal{C}$ . Then, by defining  $g_k := |h_{x_k}|^2$  and  $I = \sum_{k>n} g_k \gamma_k^{-1}$ , the coverage probability can be written as:

$$\begin{aligned} P_n &= \mathbb{P}(\text{SINR} > \theta) \\ &= \mathbb{P}\left(\left|\sum_{k \leq n} \gamma_k^{-1/2} h_{x_k}\right|^2 > \theta \left(\sum_{k>n} g_k \gamma_k^{-1} + \sigma^2\right)\right) \\ &\stackrel{(a)}{=} E_{\gamma, I} \left( \exp\left(-\frac{\theta(I + \sigma^2)}{\sum_{k=1}^n \gamma_k^{-1}}\right) \right) \end{aligned}$$

$$\begin{aligned} &\stackrel{(b)}{=} E_{\gamma} \left( \mathcal{L} \left( \frac{\theta}{\sum_{k=1}^n \gamma_k^{-1}} \right) \exp\left(-\frac{\theta \sigma^2}{\sum_{k=1}^n \gamma_k^{-1}}\right) \right) \\ &= \int_{\substack{0 < \gamma_1 < \dots \\ \dots < \gamma_n < \infty}} \mathcal{L} \left( \frac{\theta}{\sum_{k=1}^n \gamma_k^{-1}} \right) \exp\left(-\frac{\theta \sigma^2}{\sum_{k=1}^n \gamma_k^{-1}}\right) f_{\Gamma}(\gamma) d\gamma, \end{aligned} \quad (36)$$

where (a) follows from the fact that  $|\sum_{k \leq n} \gamma_k^{-1/2} h_{x_k}|^2$  is exponentially distributed with mean  $\sum_{k=1}^n \gamma_k^{-1}$  because of the Rayleigh fading assumption, and the fact that  $(h_{x_1}, \dots, h_{x_n})$  are mutually independent, while (b) makes use of the Laplace transform of  $I$ ,  $\mathcal{L}(s) = E(e^{-sI})$ . The joint distribution of  $\gamma$  can be obtained by following the similar steps as in the derivation of the joint distribution of the nearest points in a homogeneous PPP [38]. It can be easily verified that for any  $0 < \gamma_1 < \dots < \gamma_n < \infty$ , the joint distribution of  $\gamma$  is given by

$$f_{\Gamma}(\gamma) = \left(\pi \delta \sum_{i=1}^K \lambda_i P_i^{\delta}\right)^n e^{-\pi \sum_{i=1}^K \lambda_i P_i^{\delta} \gamma_n^{\delta}} \prod_{i=1}^n \gamma_i^{\delta-1}, \quad (37)$$

where  $\delta = 2/\alpha$ .

For a given  $\gamma_n$ , notice that the Laplace transform of  $I$  can be re-written as

$$\begin{aligned} \mathcal{L}(s) &= E(e^{-sI}) \\ &\stackrel{(a)}{=} E\left(e^{-s \sum_{k>n} g_k \gamma_k^{-1}}\right) \\ &= E_{\Xi} \left( \prod_{k>n} E_{g_k} \left( e^{-s g_k \gamma_k^{-1}} \right) \right) \\ &\stackrel{(b)}{=} E_{\Xi} \left( \prod_{k>n} \frac{1}{1 + s \gamma_k^{-1}} \right) \\ &\stackrel{(c)}{=} \exp\left(-\int_{\gamma_n}^{\infty} \left[1 - \frac{1}{1 + s x^{-1}}\right] \lambda(x) dx\right) \\ &\stackrel{(d)}{=} \exp\left(-2\pi \sum_{i=1}^K \lambda_i (s P_i)^{\delta} F((\gamma_n s^{-1})^{\delta/2})\right), \end{aligned} \quad (38)$$

where (a) uses the definition of  $I$ ; (b) uses the expression for moment generating function of an exponential random variable; (c) is due to the probability generating functional for a PPP [37, Theorem 4.9]; (d) follows from the transformation  $x = s t^{\alpha}$  and the definition of  $F(x)$ .

Substituting (37) and (38) into (36), the coverage probability can be expressed as

$$\begin{aligned} &\int_{0 < \gamma_1 < \dots < \gamma_n < \infty} \exp\left[-2\pi \left(\frac{\theta}{\sum_{k=1}^n \gamma_k^{-1}}\right)^{\delta} \sum_{i=1}^K \lambda_i P_i^{\delta} \times \right. \\ &F\left(\left(\theta^{-1} \sum_{k=1}^n \frac{\gamma_n}{\gamma_k}\right)^{\delta/2}\right) - \pi \sum_{i=1}^K \lambda_i P_i^{\delta} \gamma_n^{\delta} - \frac{\theta \sigma^2}{\sum_{k=1}^n \gamma_k^{-1}} \left. \right] \times \\ &\prod_{i=1}^n \left( \sum_{j=1}^K \pi \lambda_j \delta P_j^{\delta} \gamma_i^{\delta-1} \right) d\gamma \end{aligned}$$

$$\stackrel{(a)}{=} \int_{0 < u_1 < \dots < u_n < \infty} \exp \left[ -2 \left( \frac{\theta u_n^{1/\delta}}{\sum_{k=1}^n (u_n/u_k)^{1/\delta}} \right)^\delta \times \right. \\ \left. F \left( \left( \theta^{-1} \sum_{k=1}^n \left( \frac{u_n}{u_k} \right)^{1/\delta} \right)^{\delta/2} \right) - u_n - \frac{\theta \sigma^2 q^{-1/\delta}}{\sum_{k=1}^n u_k^{-1/\delta}} \right] d\mathbf{u}, \quad (39)$$

where (a) follows by change of variable  $u_i = \sum_{j=1}^K \lambda_j P_j^\delta \pi \gamma_i^\delta$ ,  $i = 1, \dots, n$  and using the definition of  $q$ . Now using the definitions of  $\tilde{\mathbf{u}}$  and the  $L^{1/\delta}$ -norm, we get the result in Theorem 1.

#### APPENDIX B PROOF OF THEOREM 2

In the case of a single-tier network  $\Phi$  with transmit power  $P_1 = P$  and no CSI at the cooperating BSs, (3) simplifies to

$$\text{SINR} = \frac{P |\sum_{x \in \mathcal{C}} \|x\|^{-\alpha/2} h_x|^2}{P I_1 + \sigma^2}, \quad (40)$$

where  $\mathcal{C} \subset \{x_1, x_2, x_3\}$ . Recall that  $\|x_1\| = \|x_2\| = \|x_3\|$  since the Voronoi vertex is equidistant from three BSs. Let  $D = \|x_i\|$  for  $i = 1, 2, 3$ . It is proved in [39] that  $D$ 's pdf is given by

$$f_D(d) = 2(\lambda\pi)^2 d^3 e^{-\lambda\pi d^2}, \quad d \geq 0. \quad (41)$$

By defining  $g_i = |h_{x_i}|^2$ , the coverage probability  $P_n$  can be written as:

$$P_n = \mathbb{P}(\text{SINR} > \theta)$$

$$= \mathbb{P} \left( \left| \sum_{i \leq n} h_{x_i} D^{-\alpha/2} \right|^2 > \theta \left( \sum_{i > n} g_i \|x_i\|^{-\alpha} + \sigma^2/P \right) \right).$$

From the Rayleigh fading assumption, it follows that  $g_i$  and  $|\sum_{i \leq n} h_{x_i} D^{-\alpha/2}|^2$  are exponentially distributed with means 1 and  $nD^{-\alpha}$ , respectively. Therefore, by invoking the Laplace transform of  $I_1$

$$\begin{aligned} P_n &= \mathbb{E}_{D,I} \left( \exp \left( -\frac{\theta(I_1 + \sigma^2/P)}{nD^{-\alpha}} \right) \right) \\ &= \mathbb{E}_D \left( \mathcal{L} \left( \frac{\theta D^\alpha}{n} \right) \exp \left( -\frac{\theta \sigma^2 D^\alpha}{nP} \right) \right) \\ &= \int_0^\infty \mathcal{L} \left( \frac{\theta d^\alpha}{n} \right) \exp \left( -\frac{\theta \sigma^2 d^\alpha}{nP} \right) f_D(d) dd. \end{aligned} \quad (42)$$

Next, for a given  $D = d$ , the Laplace transform of  $I_1$  can be computed as

$$\begin{aligned} \mathcal{L}(s) &= \mathbb{E} \left( e^{-s I_1} \right) \\ &= \mathbb{E} \left( e^{-s \sum_{i > n} g_i \|x_i\|^{-\alpha}} \right) \\ &= \mathbb{E}_\Phi \left( \prod_{i > n} \mathbb{E}_{g_i} \left( e^{-s g_i \|x_i\|^{-\alpha}} \right) \right) \\ &\stackrel{(a)}{=} \left( \frac{1}{1 + s d^{-\alpha}} \right)^{3-n} \mathbb{E}_\Phi \left( \prod_{i > 3} \frac{1}{1 + s \|x_i\|^{-\alpha}} \right) \\ &\stackrel{(b)}{=} \left( \frac{1}{1 + s d^{-\alpha}} \right)^{3-n} e^{-2\pi \int_d^\infty \left[ 1 - \frac{1}{1 + s x^{-\alpha}} \right] \lambda x dx} \end{aligned}$$

$$\stackrel{(c)}{=} \left( \frac{1}{1 + s d^{-\alpha}} \right)^{3-n} e^{-2\pi \lambda s^{2/\alpha} F(d s^{-1/\alpha})}, \quad (43)$$

where (a) uses the expression for the moment generating function of an exponential random variable; (b) is due to the probability generating functional for a PPP [37, Theorem 4.9]; (c) follows from the transformation  $x = t s^{1/\alpha}$  and the definition of  $F(x)$ . Finally, substituting (43) and (41) into (42) gives us the desired result.

#### APPENDIX C PROOF OF PROPOSITION 1

We only prove the claim for Case 1 since a similar argument applies to Case 2. Following the notations in Appendix A,  $\text{SINR}_D$  in (29) can be re-written as

$$\text{SINR}_D = \frac{\left| \sum_{k \leq n} \gamma_k^{-1/2} h_k \right|^2}{\left| \sum_{k \in \mathcal{I}_D} \gamma_k^{-1/2} h_k \right|^2 + \sum_{k \in \mathcal{I}_D^c} \gamma_k^{-1} g_k}, \quad (44)$$

where  $\gamma_k$  is defined in (35),  $\mathcal{I}_D$  denotes the index set of BSs in  $D$  and  $\mathcal{I}_D^c$  denotes the index set of the remaining interferers. Following similar steps as in (36),  $\mathbb{P}(\text{SINR}_D > \theta)$  can be expressed as

$$\int_{\substack{0 < \gamma_1 < \dots \\ \dots < \gamma_n < \infty}} \mathcal{L}_D \left( \frac{\theta}{\sum_{k=1}^n \gamma_k^{-1}} \right) \exp \left( -\frac{\theta \sigma^2}{\sum_{k=1}^n \gamma_k^{-1}} \right) f_\Gamma(\gamma) d\gamma, \quad (45)$$

where

$$\begin{aligned} \mathcal{L}_D(s) &= \mathbb{E} \left( e^{-s \left( \left| \sum_{k \in \mathcal{I}_D} \gamma_k^{-1/2} h_k \right|^2 + \sum_{k \in \mathcal{I}_D^c} \gamma_k^{-1} g_k \right)} \right) \\ &\stackrel{(a)}{=} \mathbb{E}_\Xi \left( \mathbb{E}_h \left( e^{-s \left| \sum_{k \in \mathcal{I}_D} \gamma_k^{-1/2} h_k \right|^2} \right) \prod_{k \in \mathcal{I}_D^c} \mathbb{E}_{g_k} \left( e^{-s g_k \gamma_k^{-1}} \right) \right) \\ &\stackrel{(b)}{=} \mathbb{E}_\Xi \left( \frac{1}{1 + s \sum_{k \in \mathcal{I}_D} \gamma_k^{-1}} \prod_{k \in \mathcal{I}_D^c} \frac{1}{1 + s \gamma_k^{-1}} \right). \end{aligned} \quad (46)$$

Here, (a) follows from the independence of the fading coefficients and (b) follows from the fact that  $\left| \sum_{k \in \mathcal{I}_D} \gamma_k^{-1/2} h_k \right|^2$  is exponentially distributed with mean  $\sum_{k \in \mathcal{I}_D} \gamma_k^{-1}$ . Using the fact that  $\frac{1}{1 + s \sum_{k \in \mathcal{I}_D} \gamma_k^{-1}} > \prod_{k \in \mathcal{I}_D} \frac{1}{1 + s \gamma_k^{-1}}$  for  $s \in \mathbb{R}^+$ , we can write

$$\begin{aligned} \mathcal{L}_D \left( \frac{\theta}{\sum_{j=1}^n \gamma_j^{-1}} \right) &\geq \mathbb{E}_\Xi \left( \prod_{k \in \mathcal{I}_D \cup \mathcal{I}_D^c} \frac{1}{1 + \frac{\theta}{\sum_{j=1}^n \gamma_j^{-1}} \gamma_k^{-1}} \right) \\ &= \mathcal{L}_\emptyset \left( \frac{\theta}{\sum_{j=1}^n \gamma_j^{-1}} \right), \end{aligned} \quad (47)$$

where the equality holds iff  $D = \emptyset$ . By combining (45) and (47), the result follows.

APPENDIX D  
PROOF OF PROPOSITION 3

We proceed by following the same steps as in Appendix A. First, we map  $\Phi_i^{(o)}$  and  $\Phi_i^{(c)}$  to the normalized path loss processes  $\Xi_i^{(o)} = \{\|x\|^\alpha/P_i, x \in \Phi_i^{(o)}\}$  and  $\Xi_i^{(c)} = \{\|x\|^\alpha/P_i, x \in \Phi_i^{(c)}\}$ . By the mapping theorem, these are non-homogeneous PPPs with intensities  $\lambda_i^{(o)}(x) = \lambda_i p_i \frac{2\pi}{\alpha} P_i^{2/\alpha} x^{2/\alpha-1}$  and  $\lambda_i^{(c)}(x) = \lambda_i(1-p_i) \frac{2\pi}{\alpha} P_i^{2/\alpha} x^{2/\alpha-1}$ . Next, we define the non-homogeneous PPP processes  $\Xi^{(o)} = \bigcup_{i=1}^K \Xi_i^{(o)}$  and  $\Xi^{(c)} = \bigcup_{i=1}^K \Xi_i^{(c)}$  and reorder their elements in increasing order of magnitude. We denote  $\gamma_k^{(o)} := \|x_k\|^\alpha/P_{\nu(x_k)}$ ,  $x_k \in \bigcup_{i=1}^K \Phi_i^{(o)}$  and  $\gamma_k^{(c)} := \|x_k\|^\alpha/P_{\nu(x_k)}$ ,  $x_k \in \bigcup_{i=1}^K \Phi_i^{(c)}$  the  $k$ th elements in these ordered lists.

By defining  $g_k^{(o)} := |h_{x_k}|^2$ ,  $x_k \in \bigcup_{i=1}^K \Phi_i^{(o)}$ ;  $g_k^{(c)} := |h_{x_k}|^2$ ,  $x_k \in \bigcup_{i=1}^K \Phi_i^{(c)}$ ;  $I = \sum_{k>n} g_k^{(o)} \gamma_k^{(o)-1} + \sum_{k=1}^\infty g_k^{(c)} \gamma_k^{(c)-1}$  and  $\gamma^{(o)} = \{\gamma_1^{(o)}, \dots, \gamma_n^{(o)}\}$ , the coverage probability in (8) with  $\sigma^2 = 0$  can be re-written as:

$$P_n = \int_{\substack{0 < \gamma_1^{(o)} < \dots \\ \dots < \gamma_n^{(o)} < \infty}} \mathcal{L} \left( \frac{\theta}{\sum_{k=1}^n \gamma_k^{(o)-1}} \right) f_{\Gamma^{(o)}}(\gamma^{(o)}) d\gamma^{(o)} \quad (48)$$

where  $f_{\Gamma^{(o)}}(\gamma)$  is given by (37) with  $\lambda_i$  replaced with  $\lambda_i p_i$  and  $\mathcal{L}(s) = \mathbb{E}(e^{-sI})$  which can be further expressed as

$$\begin{aligned} \mathcal{L}(s) &= \mathbb{E}(e^{-sI}) \\ &\stackrel{(a)}{=} \mathbb{E}_{\Xi^{(o)}, \Xi^{(c)}} \left( e^{-s \sum_{k>n} g_k^{(o)} \gamma_k^{(o)-1} - s \sum_{k=1}^\infty g_k^{(c)} \gamma_k^{(c)-1}} \right) \\ &\stackrel{(b)}{=} \mathbb{E}_{\Xi^{(o)}} \left( \prod_{k>n} \mathbb{E}_{g_k^{(o)}} \left( e^{-s g_k^{(o)} \gamma_k^{(o)-1}} \right) \right) \\ &\quad \times \mathbb{E}_{\Xi^{(c)}} \left( \prod_{k=1}^\infty \mathbb{E}_{g_k^{(c)}} \left( e^{-s g_k^{(c)} \gamma_k^{(c)-1}} \right) \right) \\ &= \mathbb{E}_{\Xi^{(o)}} \left( \prod_{k>n} \frac{1}{1 + s \gamma_k^{(o)-1}} \right) \\ &\quad \times \mathbb{E}_{\Xi^{(c)}} \left( \prod_{k=1}^\infty \frac{1}{1 + s \gamma_k^{(c)-1}} \right) \\ &\stackrel{(c)}{=} \exp \left( - \int_{\gamma_n}^\infty \left[ 1 - \frac{1}{1 + s x^{-1}} \right] \lambda^{(o)}(x) dx \right) \\ &\quad \times \exp \left( - \int_0^\infty \left[ 1 - \frac{1}{1 + s x^{-1}} \right] \lambda^{(c)}(x) dx \right) \\ &\stackrel{(d)}{=} \exp \left( -2\pi \sum_{i=1}^K \lambda_i p_i (s P_i)^{2/\alpha} F((\gamma_n s^{-1})^{1/\alpha}) \right) \\ &\quad \times \exp \left( -\pi \sum_{i=1}^K \lambda_i (1-p_i) (s P_i)^{2/\alpha} / \text{sinc}(2/\alpha) \right), \end{aligned} \quad (49)$$

where (a) uses the definition of  $I$ ; (b) uses the independence of  $\Xi^{(o)}$  and  $\Xi^{(c)}$ ; (c) is due to the probability generating functional for a PPP; (d) follows from the change of variable  $x = s t^\alpha$  and the definition of  $F(x)$ .

Finally, the claim follows by substituting (37) (with  $\lambda_i$  replaced by  $\rightarrow \lambda_i p_i$ ) and (49) into (48), and by perform-

ing the change of variable  $u_i = \sum_{j=1}^K \lambda_j p_j P_j^{2/\alpha} \pi \gamma_i^{(o)2/\alpha}$ ,  $i = 1, \dots, n$ .

REFERENCES

- [1] Cisco, "Cisco visual networking index: Global mobile data traffic forecast update, 2012-2017," white paper, Tech. Rep., February 2013.
- [2] D. Lee, H. Seo, B. Clerckx, E. Hardouin, D. Mazzaresse, S. Nagata, and K. Sayana, "Coordinated multipoint transmission and reception in LTE-Advanced: deployment scenarios and operational challenges," *IEEE Communications Magazine*, vol. 50, no. 2, pp. 148–155, February 2012.
- [3] G. Foschini, K. Karakayali, and R. Valenzuela, "Coordinating multiple antenna cellular networks to achieve enormous spectral efficiency," *IEEE Proceedings in Communications*, vol. 153, no. 4, pp. 548–555, August 2006.
- [4] M. Sawahashi, Y. Kishiyama, A. Morimoto, D. Nishikawa, and M. Mayer, "Coordinated multipoint transmission/reception techniques for LTE-Advanced [coordinated and distributed MIMO]," *IEEE Wireless Communications*, vol. 17, no. 3, pp. 26–34, June 2010.
- [5] R. Irmer, H. Droste, P. Marsch, M. Grieger, G. Fettweis, S. Brueck, H.-P. Mayer, L. Thiele, and V. Jungnickel, "Coordinated multipoint: Concepts, performance, and field trial results," *IEEE Communications Magazine*, vol. 49, no. 2, pp. 102–111, February 2011.
- [6] S. Brueck, L. Zhao, J. Giese, and M. A. Amin, "Centralized scheduling for joint transmission coordinated multi-point in LTE-Advanced," *International ITG Workshop on Smart Antennas*, pp. 177–184, February 2010.
- [7] E. Hossain, D. I. Kim, and V. K. Bhargava, *Cooperative Cellular Wireless Networks*. Cambridge University Press, 2011.
- [8] S. Shamai and B. Zaidel, "Enhancing the cellular downlink capacity via co-processing at the transmitting end," in *53rd IEEE Vehicular Technology Conference*, vol. 3, May 2001, pp. 1745–1749.
- [9] O. Somekh, B. Zaidel, and S. Shamai, "Sum rate characterization of joint multiple cell-site processing," *IEEE Trans. Inf. Theory*, vol. 53, no. 12, pp. 4473–4497, December 2007.
- [10] S. Jing, D. N. C. Tse, J. B. Soriaga, J. Hou, J. E. Smee, and R. Padovani, "Multicell downlink capacity with coordinated processing," *EURASIP J. Wireless Comm. and Networking*, vol. 2008, April 2008.
- [11] O. Simeone, O. Somekh, H. Poor, and S. Shamai, "Local base station cooperation via finite-capacity links for the uplink of linear cellular networks," *IEEE Trans. Inf. Theory*, vol. 55, no. 1, pp. 190–204, January 2009.
- [12] A. Wyner, "Shannon-theoretic approach to a Gaussian cellular multiple-access channel," *IEEE Trans. Inf. Theory*, vol. 40, no. 6, pp. 1713–1727, November 1994.
- [13] J. Xu, J. Zhang, and J. G. Andrews, "On the accuracy of the Wyner model in cellular networks," *IEEE Transactions on Wireless Communications*, vol. 10, no. 9, pp. 3098–3109, September 2011.
- [14] D. Gesbert, S. Hanly, H. Huang, S. S. Shitz, O. Simeone, and W. Yu, "Multi-cell MIMO cooperative networks: A new look at interference," *IEEE Journal on Selected Areas in Communications*, vol. 28, no. 9, pp. 1380–1408, December 2010.
- [15] A. Lozano, R. W. Heath, and J. G. Andrews, "Fundamental limits of cooperation," *IEEE Transactions on Information Theory*, vol. 59, no. 9, pp. 5213–5226, September 2013.
- [16] H. ElSawy, E. Hossain, and M. Haenggi, "Stochastic geometry for modeling, analysis, and design of multi-tier and cognitive cellular wireless networks: A survey," *IEEE Communications Surveys & Tutorials*, vol. 15, no. 3, pp. 996–1019, July 2013.
- [17] M. Haenggi, J. Andrews, F. Baccelli, O. Dousse, and M. Franceschetti, "Stochastic geometry and random graphs for the analysis and design of wireless networks," *IEEE Journal on Selected Areas in Communications*, vol. 27, no. 7, pp. 1029–1046, September 2009.
- [18] H. S. Dhillon, R. K. Ganti, F. Baccelli, and J. G. Andrews, "Modeling and analysis of K-tier downlink heterogeneous cellular networks," *IEEE Journal on Selected Areas in Communications*, vol. 30, no. 3, pp. 550–560, April 2012.
- [19] L. Wu, Y. Zhong, and W. Zhang, "Spatial statistical modeling for heterogeneous cellular networks - an empirical study," *IEEE Vehicular Technology Conference (VTC2014-Spring)*, Seoul, Korea, May 2014.
- [20] M. D. Renzo, A. Guidotti, and G. Corazza, "Average rate of downlink heterogeneous cellular networks over generalized fading channels: a stochastic geometry approach," *IEEE Transactions on Communications*, vol. 61, no. 7, pp. 3050–3071, July 2013.

- [21] P. Xia, C.-H. Liu, and J. G. Andrews, "Downlink coordinated multi-point with overhead modeling in heterogeneous cellular networks," *IEEE Transactions on Wireless Communications*, vol. 12, no. 8, pp. 4025–4037, August 2013.
- [22] A. Giovanidis and F. Baccelli, "A stochastic geometry framework for analyzing pairwise-cooperative cellular networks," May 2013, submitted. [Online]. Available: <http://arxiv.org/abs/1305.6254>
- [23] F. M. J. Willems, "The discrete memoryless multiple access channel with partially cooperating encoders," *IEEE Trans. Inf. Theory*, vol. 29, no. 3, pp. 441–445, May 1983.
- [24] S. Akoum and R. Heath, "Multi-cell coordination: A stochastic geometry approach," in *IEEE 13th International Workshop on Signal Processing Advances in Wireless Communications*, June 2012, pp. 16–20.
- [25] R. Tanbourgi, S. Singh, J. G. Andrews, and F. K. Jondral, "Analysis of non-coherent joint-transmission cooperation in heterogeneous cellular networks," *IEEE International Conference on Communications, Sydney, Australia*, June 2014. [Online]. Available: <http://arxiv.org/pdf/1402.2707v2.pdf>
- [26] X. Zhang and M. Haenggi, "A stochastic geometry analysis of inter-cell interference coordination and intra-cell diversity," *IEEE Transactions on Wireless Communications*, 2013, submitted. [Online]. Available: <http://www.nd.edu/~mhaenggi/pubs/twc14b.pdf>
- [27] D. Tse and P. Viswanath, *Fundamentals of Wireless Communication*. Cambridge University Press, 2005.
- [28] S. Mukherjee, "Distribution of downlink sinr in heterogeneous cellular networks," *IEEE Journal on Selected Areas in Communications*, vol. 30, no. 3, pp. 575–585, 2012.
- [29] J. G. Andrews, F. Baccelli, and R. K. Ganti, "A tractable approach to coverage and rate in cellular networks," *IEEE Transactions on Communications*, vol. 59, no. 11, pp. 3122–3134, November 2011.
- [30] H. Wang and M. C. Reed, "A novel tractable framework to analyse heterogeneous cellular networks," in *IEEE GLOBECOM Workshops (GC Wkshps)*, 2011, 2011, pp. 287–292.
- [31] S. Y. Jung, H. K. Lee, and S. L. Kim, "Worst-case user analysis in Poisson Voronoi cells," *IEEE Communications Letters*, vol. 17, no. 8, pp. 1580–1583, August 2013.
- [32] G. Nigam, P. Minero, and M. Haenggi, "Proof of finiteness in Theorem 5," 2014. [Online]. Available: <http://www3.nd.edu/~mhaenggi/pubs/techreport14b.pdf>
- [33] I. Gradshteyn and I. Ryzhik, *Table of Integrals, Series, and Products*, 7th ed. Academic Press, 2007.
- [34] A. Guo and M. Haenggi, "Asymptotic deployment gain: A new approach to characterize coverage probability," *IEEE International Conference on Communications, Sydney, Australia*, June 2014.
- [35] X. Zhang and M. Haenggi, "The performance of successive interference cancellation in random wireless networks," *IEEE Transactions on Information Theory*, 2013, submitted. Available at <http://www.nd.edu/~mhaenggi/pubs/tit14.pdf>.
- [36] 3GPP, "3GPP TS 36.423 V10.1.0 (2011-03) X2 application protocol (X2AP)," technical Specification, 2011.
- [37] M. Haenggi, *Stochastic Geometry for Wireless Networks*. Cambridge University Press, 2013.
- [38] D. Moltchanov, "Survey paper: Distance distributions in random networks," *Ad Hoc Networks*, vol. 10, no. 6, pp. 1146–1166, August 2012.
- [39] V. Baumstark and G. Last, "Some distributional results for Poisson-Voronoi tessellations," in *Advances in Applied Probability*. Applied Probability Trust, March 2007, vol. 39, no. 1, pp. 16–40.